Pergamon

0301-9322(94)00049-2

Int. J. Multiphase Flow Vol. 20, No. 6, pp. 1129–1142, 1994
Elsevier Science Ltd.
Printed in Great Britain

EFFECTS OF DOUBLE-HUMPED AXIAL HEAT FLUX VARIATION ON THE STABILITY OF TWO-PHASE FLOW IN HEATED CHANNELS

RIZWAN-UDDIN

Department of Mechanical, Aerospace and Nuclear Engineering, University of Virginia, Charlottesville, VA 22903-2442, U.S.A.

(Received 18 May 1993; in revised form 28 April 1994)

Abstract—Stability analysis of two-phase flow in heated channels with double-humped axial heat flux variation, relevant to boiling water nuclear reactors, has been carried out. Single-phase and two-phase flow equations are linearized about the steady-state solution, and the stability of the fixed points is studied in frequency domain. Effects of symmetric and asymmetric double-humped axial heat flux variation on stability has been determined. Results are presented as stability boundaries in parameter space and as bifurcation diagrams. It is found that whether a channel with single-humped heat flux variation becomes more or less stable as the heat flux is replaced by an equivalent double-humped profile, actually depends upon other system parameters, such as the channel inlet subcooling. For example, for low inlet subcooling, a channel with symmetric double-humped heat flux variation is less stable than another channel with single-humped heat flux variation (same total heat flux), whereas, the trend is reversed for high inlet subcooling.

Key Words: two-phase flow, parallel channel flow, density-wave oscillations, stability, double-humped axial heat flux

INTRODUCTION

Sustained flow oscillations occur in heated two-phase flow systems, such as heat exchangers, cryogenic equipment, chemical plants, boiling water nuclear reactors (BWR), etc. Associated vibrations and thermal fatigue can be very detrimental to the safe operation of these equipment. Such instabilities are characterized by a delayed pressure drop response in the two-phase region to any variation at the system inlet. Although the oscillation mechanism in boiling water nuclear reactors is even more complex due to additional feedback between the two-phase thermal hydraulics and neutron kinetics—via void fraction, neutron thermalization and heat generation—the fundamental cause of instability is still the characteristic single- and two-phase delayed pressure drop in the heated channel. These instabilities have been studied extensively in experimental set ups, and analyzed using analytical and numerical techniques over the last three decades (Stenning & Veziroğlu 1965; Bouré *et al.* 1973; Saha *et al.* 1976; Bouré 1978; Ünal 1981; Lorenzini 1981; Achard *et al.* 1985; Rizwan-uddin & Dorning 1986, 1987, 1988; Clause *et al.* 1989; Xiao *et al.* 1993). Analysis of density-wave oscillations in complex systems by *numerical* simulation of space and time-dependent thermal hydraulics (or neutron kinetics coupled thermal hydraulics, in case of BWRs) is time consuming and computationally very expensive. Moreover, effects of various design and operating parameters on stability are relatively difficult to evaluate numerically. Hence, frequency domain linear and if possible, nonlinear analyses—even if carried out for special simpler cases—are extremely valuable. Results of such analyses show the effects of design and operating parameters on stability, and also help in efficient and systematic 'combing' of the parameter space when more detailed and time consuming numerical codes must be used.

Frequency domain stability analyses of heated channels with two-phase flow have so far been restricted to channels with either axially uniform heat fluxes (Stenning & Veziroğlu 1965; Saha *et al.* 1976; Achard *et al.* 1985; Rizwan-uddin & Dorning 1986), or in case of axially varying heat flux, to channels with heat flux with a single-hump, such as represented by $q''(z) = q''_0 \sin(a + bz)$ (Rizwan-uddin & Dorning 1987). Though the single-humped heat flux profile is realistic for many cases, various other heat flux profiles, especially double-humped axial heat flux, may result in engineering equipment. Boiling water nuclear reactors, due to their characteristic feedback

mechanism among void fraction, neutron thermalization and heat generation, coupled with long term depletion effects, are specially likely to have double-humped axial heat flux shapes (Valtonen 1989). Moreover, flow and flux oscillation problems experienced by some BWRs have brought increased attention to their stability characteristics (Sandoz & Chen 1983; Diederich 1988; Bergdahl *et al.* 1989; Araya *et al.* 1991). In fact, data from the plant recorder from one such incident shows that at the time oscillations started at LaSalle-2 (Diederich 1988), the axial power profile in the reactor core was actually asymmetric (bottom peaked) and double-humped (Wulff *et al.* 1991). It is later shown in this paper that analysis of the stability characteristics of a channel with realistic double-humped axial heat flux variation, as a uniformly heated channel or as a channel with a single hump in axial heat flux, may lead to non-conservative conclusions. Hence, results of previous studies, carried out for uniformly heated channels and for heated channels with a single hump, cannot be used to analyze heated channels with double-humped axial heat flux profiles, indicating the need for detailed stability analysis of the latter and the need to study the parametric effects on their stability.

In this work, to study the stability characteristics of two-phase flow heated channels with double-humped heat flux profiles, frequency domain analysis has been carried out using the homogeneous equilibrium model to represent the two-phase flow (Lorenzini 1981; Achard *et al.* 1985; Clause *et al.* 1989; Frutera 1986). [The effect of using the drift flux model on the stability characteristics of uniformly heated channels has already been studied (Rizwan-uddin & Dorning 1986), and it is realized that though the drift flux model is important, the salient features of the stability characteristics of heated channels with two humps in heat flux profile can be studied using the homogeneous equilibrium model (Frutera 1986).]

We start with the sets of partial differential equations (PDEs) for the single-phase and two-phase regions of the heated channel. After tranforming the two sets of PDEs to dimensionless variables, the steady-state solutions or the fixed points of the system are first calculated. Next, the equations are linearized about the fixed points and the set of resulting linear PDEs is solved to determine the characteristic equation. System stability is then determined in parameter space by the roots of the characteristic equation.

MODEL

Figure 1 schematically shows a heated channel of length L^* with smoothly varying axial heat flux profile given by $q''^*(z) \equiv q_0''^* f(z)$. [(*)s represent a dimensional quantity and will be dropped once these quantities are made dimensionless.] The flow is due to an externally imposed pressure drop ΔP_{ex}^*, and the resulting inlet velocity (a dependent variable) is $v_i^*(t^*)$. Liquid is subcooled at the inlet and the inlet temperature T_i^* (or enthalpy h_i^*) is also specified.

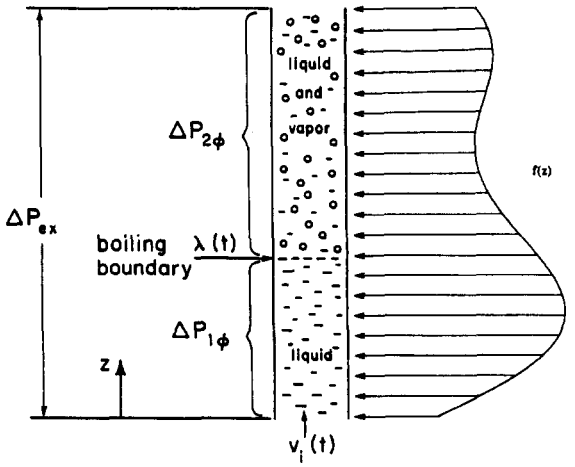

Figure 1. Schematic diagram of a heated channel with two-phase flow. Heat flux is given by $q''(z) = q_0'' f(z)$. Channel length is L, inlet temperature T_i, inlet velocity $v_i(t)$, and the flow is due to an externally imposed pressure drop ΔP_{ex}.

The heated channel is divided into single-phase region and two-phase region. Axial location where boiling starts—boundary between single-phase and two phase regions—is called the boiling boundary and is denoted by $\lambda^*(t^*)$. Assuming incompressible liquid phase, the velocity throughout the single-phase region is equal to the inlet velocity. Hence, mass, momentum and energy conservation equations in the single-phase region are $(0 < z^* < \lambda^*(t^*))$

$$\rho_L^*(z^*, t^*) = \rho_L^* = constant$$

$$v_i^*(z^*, t^*) = v_i^*(t^*) \quad [1]$$

$$-\frac{\partial P_{1\phi}^*}{\partial z^*} = \rho_L^* \frac{dv_i^*(t^*)}{dt^*} + \rho_L^* \frac{f_s^*(v_i^*(t^*))^2}{2D^*} + \rho_L^* g^* \quad [2]$$

$$\frac{\partial h^*(z^*, t^*)}{\partial t^*} + v_i^*(t^*) \frac{\partial h^*(z^*, t^*)}{\partial z^*} = q_0''^* f(z) \quad [3]$$

where subscript i is used to denote quantities at the channel inlet, and subscripts 1ϕ and 2ϕ represent single-phase and two-phase flow quantities. Note that the boiling boundary $\lambda^*(t^*)$ is the axial location at which enthalpy $h^*(z^*, t^*)$ is equal to the saturation enthalpy h_{sat}^*

$$h^*(z^* = \lambda^*(t^*), t^*) = h_{sat}^*. \quad [4]$$

The homogeneous equilibrium model for the two-phase flow is characterized by mixture velocity (or volumetric flux) $j^*(z^*, t^*)$, and mixture density $\rho_m^*(z^*, t^*)$. The equations for j^*, ρ_m^* and two-phase region pressure drop $\Delta P_{2\phi}^*$ are (Zuber & Findley 1965; Zuber & Staub 1967)

$$\frac{\partial j^*(z^*, t^*)}{\partial z^*} = \frac{\Gamma_G^* \Delta \rho^*}{\rho_G^* \rho_L^*} f(z), \quad [5]$$

$$\frac{\partial \rho_m^*(z^*, t^*)}{\partial t^*} + j^*(z^*, t^*) \frac{\partial \rho_m^*}{\partial z^*} = \frac{-\Gamma_G^*}{\rho_G^*} f(z) \Delta \rho^* \rho_m^*(z^*, t^*) \quad [6]$$

$$\rho_m^* \left(\frac{\partial j^*}{\partial t^*} + j^* \frac{\partial j^*}{\partial z^*} \right) = -\frac{\partial P_{2\phi}^*}{\partial z^*} - \frac{f_m^*}{2D^*} \rho_m^* j^{*2} - g^* \rho_m^* \quad [7]$$

where

$$\Gamma_G^* \equiv \frac{q_0''^* \xi^*}{\Delta h_{LG}^* A^*} \quad [8]$$

and void fraction and mixture density are related by

$$\epsilon^*(z^*, t^*) = \left(1 - \frac{\rho_m^*(z^*, t^*)}{\rho_L^*} \right) \frac{\rho_L^*}{\Delta \rho^*}, \quad [9]$$

where ξ^* is the heated perimeter, A^* is the flow area and, $\rho_m^*(z^*, t^*)$ and $j^*(z^*, t^*)$ are mixture density and mixture velocity, respectively. Pressure drops at the inlet and exit of the heated channel are given by

$$\Delta P_i^*(t^*) = k_i \rho_L^* v_i^{*2}(t^*) \quad [10]$$

$$\Delta P_e^*(t^*) = k_e \rho_m^*(z^* = L^*, t^*) j^{*2}(z^* = L^*, t^*) \quad [11]$$

where k_i and k_e are the inlet and exit pressure drop coefficients, respectively.

Using the dimensionless variables and parameters given in appendix A (Rizwan-uddin & Dorning 1986), the above set of equations is made dimensionless. The resulting equations for the single-phase region $(0 < z < \lambda(t))$ are

$$\rho_m(z, t) = \rho_L(z, t) = 1,$$

$$j(z, t) = v_L(z, t) = v_i(z, t) = v_i(t) \quad [12]$$

$$\frac{\partial h(z, t)}{\partial t} + v_i(t) \frac{\partial h(z, t)}{\partial z} = N_{pch} \left(\frac{N_\rho}{1 - N_\rho} \right) f(z) \quad [13]$$

$$-\frac{\partial P_{1\phi}}{\partial z} = \frac{\mathrm{d}v_i(t)}{\mathrm{d}t} + N_{f1}v_i^2(t) + Fr^{-1}. \quad [14]$$

Similarly, the dimensionless equations for the two-phase region ($\lambda(t) < z < 1$) are,

$$\frac{\partial j(z,t)}{\partial z} = N_{\mathrm{pch}} f(z), \quad [15]$$

$$\frac{\partial \rho_m(z,t)}{\partial t} + j(z,t)\frac{\partial \rho_m(z,t)}{\partial z} = -N_{\mathrm{pch}}\rho_m(z,t)f(z), \quad [16]$$

$$-\frac{\partial P_{2\phi}}{\partial z} = \rho_m(z,t)\left(\frac{\partial j(z,t)}{\partial t} + j(z,t)\frac{\partial j(z,t)}{\partial z} + Fr^{-1} + N_{f2}j^2(z,t)\right) \quad [17]$$

and

$$\epsilon(z,t) = (1 - \rho_m(z,t))N_r. \quad [18]$$

Single-phase and two-phase region momentum equations when integrated over their respective region lengths yield,

$$\Delta P_{1\phi}(t) = \left(\frac{\mathrm{d}v_i(t)}{\mathrm{d}t} + N_{f1}v_i^2(t) + Fr^{-1}\right)\lambda(t), \quad [19]$$

$$\Delta P_{2\phi}(t) = \int_{\lambda(t)}^{1} \rho_m(z,t)\left[\frac{\partial j(z,t)}{\partial t} + j\frac{\partial j(z,t)}{\partial z} + Fr^{-1} + N_{f2}j^2(z,t)\right]\mathrm{d}z. \quad [20]$$

Dimensionless pressure drop at the channel inlet and exit are

$$\Delta P_i(t) = k_i v_i^2(t) \quad [21]$$

$$\Delta P_e(t) = k_e \rho_m(z=1,t) j^2(z=1,t). \quad [22]$$

The dimensionless parameter 'phase change number', N_{pch}, is proportional to the amount of heat supplied to the channel. In order to compare stability characteristics of channels with different axial heat flux shapes, it will be necessary to compare them at the same total (heat) energy supplied. Hence, a 'total phase change number' $N_{\mathrm{pch,tot}}$, is defined as

$$N_{\mathrm{pch,tot}} = N_{\mathrm{pch}} \int_0^1 f(z)\,\mathrm{d}z. \quad [23]$$

Also note that when the heat flux profile $f(z)$ is taken as one, the model developed above reduces to that of a heated channel with uniform axial heat flux along the channel length. This special case ($f(z) = 1$) has already been studied (Achard *et al.* 1985; Rizwan-uddin & Dorning 1986), and the results were found to agree quite well with the experimental data of Saha *et al.* (1976).

STEADY-STATE ANALYSIS

Solution of the time-independent problem is obtained by assuming all dependent variables to be independent of time. The energy equation in the single-phase region yields an expression for enthalpy $\tilde{h}(z)$ which results in a transcendental expression for the (steady-state) position of the boiling boundary $\tilde{\lambda}$,

$$g(\tilde{\lambda}) - g(0) = \frac{\tilde{v}N_{\mathrm{sub}}}{N_{\mathrm{pch}}} \quad [24]$$

where

$$g(z) = \int f(z)\,\mathrm{d}z,$$

$\tilde{v}$ is the steady-state inlet velocity, and the steady-state quantities are represented by an 'over tilde' (~). Note that the subscript i from the steady-state inlet velocity has been dropped. Single-phase

region pressure drop becomes

$$\tilde{\Delta}P_{1\phi} = (N_{f1}\tilde{v}^2 + Fr^{-1})\tilde{\lambda}. \quad [25]$$

In the two-phase region, volumetric flux $\tilde{j}(z)$, mixture density $\tilde{\rho}_m$, and pressure drop $\tilde{\Delta}P_{2\phi}$ are given by

$$\tilde{j}(z) = \tilde{v} + N_{pch}[g(z) - g(\tilde{\lambda})] \quad [26]$$

$$\tilde{\rho}_m(z) = \frac{\tilde{v}}{\tilde{j}(z)} \quad [27]$$

$$\tilde{\Delta}P_{2\phi} = \int_{\tilde{\lambda}}^{1} \tilde{\rho}_m(z)\left[\tilde{j}(z)\frac{d\tilde{j}(z)}{dz} + N_{f2}\tilde{j}^2(z) + Fr^{-1}\right]dz. \quad [28]$$

The steady-state concentrated pressure drops at the channel inlet and exit are as given by [21] and [22]. The equation for the total pressure drop in the channel, which is equal to the externally imposed pressure drop ΔP_{ex}, is

$$\tilde{\Delta}P_{tot} = \tilde{\Delta}P_i + \tilde{\Delta}P_e + \tilde{\Delta}P_{1\phi} + \tilde{\Delta}P_{2\phi} = \Delta P_{ex}.$$

For given geometry, inlet temperature, heat flux and externally imposed pressure drop, the last equation is used to determine the steady-state inlet velocity $\tilde{v}$.

STABILITY ANALYSIS

The vector of dependent variables is

$$y \equiv [h(z,t), \lambda(t), j(z,t), \rho_m(z,t), \Delta P_{1\phi}(t), \Delta P_{2\phi}(t), \Delta P_i(t), \Delta P_e(t)]^T.$$

We linearize the set of equations about the steady-state solution found in the previous section. Keeping only the linear terms yields the following set of differential and algebraic equations,

$$\frac{\partial \delta h(z,t)}{\partial t} + \tilde{v}\frac{\partial \delta h(z,t)}{\partial z} + \delta v(t)\frac{d\tilde{h}(z)}{dz} = 0 \quad [29]$$

$$f(\tilde{\lambda})\delta\lambda(t) + v\tilde{v}\delta h(\tilde{\lambda}, t) = 0 \quad [30]$$

$$\delta j(t) - \delta v(t) + N_{pch} f(\tilde{\lambda})\delta\lambda(t) = 0 \quad [31]$$

$$\frac{\partial \delta\phi_m(z,t)}{\partial t} + \tilde{j}(z)\frac{\partial \delta\phi_m(z,t)}{\partial z} + \delta j(t)\frac{d\tilde{\phi}_m(z)}{dz} = 0 \quad [32]$$

$$\delta\phi_m(z,t) - \frac{\delta\rho_m(z,t)}{\tilde{\rho}_m(z)} = 0 \quad [33]$$

$$\delta\Delta P_i(t) - 2k_i\tilde{v}\delta v(t) = 0 \quad [34]$$

$$\delta\Delta P_e(t) - k_e\{2\tilde{\rho}_m(z=1)\tilde{j}(z=1)\delta j(z=1,t) + \tilde{j}^2(z=1)\delta\rho_m(z=1,t)\} = 0 \quad [35]$$

$$\delta\Delta P_{1\phi}(t) - \tilde{\lambda}\frac{d\delta v(t)}{dt} - 2N_{f_1}\tilde{v}\tilde{\lambda}\delta v(t) - (N_{f_1}\tilde{v}^2 + Fr^{-1})\delta\lambda(t) = 0 \quad [36]$$

$$\delta\Delta P_{2\phi}(t) - \int_{\tilde{\lambda}}^{1} \tilde{\rho}_m(z)L^m(\delta j(z,t))\,dz - \int_{\tilde{\lambda}}^{1} S_1(z)\delta\rho_m(z,t)\,dz + S_1(\tilde{\lambda})\delta\lambda(t) = 0 \quad [37]$$

where the following definitions have been used

$$\phi_m(z,t) \equiv \ln[\rho_m(z,t)] \quad [38]$$

$$L^m(y) \equiv \left(\frac{\partial}{\partial t} + \tilde{j}(z)\frac{\partial}{\partial z} + \frac{d\tilde{j}(z)}{dz} + 2N_{f_2}\tilde{j}(z)\right)y \quad [39]$$

$$\tilde{S}_1(z) \equiv \tilde{j}(z)\frac{d\tilde{j}(z)}{dz} + N_{f_2}j^2(z) + Fr^{-1}. \quad [40]$$

The set of equations linearized about the fixed point (or steady-state) obtained above is solved

below to obtain one equation in terms of $\delta v(t)$. The stability of the steady-state solution is then analyzed using the linear equation in $\delta v(t)$.

The single-phase energy equation, [29], when integrated along the characteristics using constant inlet enthalpy boundary condition, yields

$$\delta h(z,t) = -\frac{1}{v\tilde{v}} \int_0^{z/\tilde{v}} \delta v\left(t - \frac{z}{\tilde{v}} + \eta\right) f(\tilde{v}\eta)\, d\eta, \qquad [41]$$

and when evaluated at $z = \tilde{\lambda}$, it becomes

$$\delta h(\tilde{\lambda},t) = -\frac{1}{v\tilde{v}} \int_0^{v_0} \delta v(t - v_0 + \eta) f(\tilde{v}\eta)\, d\eta \qquad [42]$$

where $v_0 \equiv \tilde{\lambda}/\tilde{v}$. Expressions for perturbation in boiling boundary $\delta\lambda(t)$ and volumetric flux $\delta j(t)$ can also be written in terms of $\delta v(t)$

$$\delta\lambda(t) = -\frac{1}{v\tilde{v}f(\tilde{\lambda})}\, \delta h(\tilde{\lambda},t) \qquad [43]$$

and

$$\delta j(t) = \delta v(t) - N_{\text{pch}} f(\tilde{\lambda})\delta\lambda(t). \qquad [44]$$

Substituting the expression for $\delta j(z,t)$ into [32] for $\delta\phi_m$, and solving the resulting linear PDE along its characteristics

$$\frac{dt}{1} = \frac{dz}{\tilde{j}(z)} = \frac{d\delta\phi_m}{-\dfrac{d\tilde{\phi}_m}{dz}\delta j(t)} \qquad [45]$$

we obtain

$$\delta\rho_m(z,t) = -\frac{N_{\text{pch}} f(\tilde{\lambda})}{\tilde{v}}\, \delta\lambda\left(t - \left(\frac{P_l(z) - P_l(\tilde{\lambda})}{N_{\text{pch}}}\right)\right) + \frac{N_{\text{pch}}}{\tilde{\rho}_m} \int_{\tilde{\lambda}}^{z} \frac{f(z')}{[\tilde{j}(z')]^2}\, \delta j\left[t - \left(\frac{P_l(z) - P_l(z')}{N_{\text{pch}}}\right)\right] dz' \qquad [46]$$

where

$$P_l(z) \equiv N_{\text{pch}} \int \frac{dz}{\tilde{j}(z)}. \qquad [47]$$

For constant external pressure drop, the sum of all individual perturbations in internal pressure drop must be equal to zero, i.e.

$$\delta\Delta P_i(t) + \delta\Delta P_e(t) + \delta\Delta P_{l\phi}(t) + \delta\Delta P_{2\phi}(t) = 0 \qquad [48]$$

Substituting the expressions from [34–37] into [48] yields

$$\tilde{\lambda}\frac{d\delta v(t)}{dt} + 2\tilde{v}(k_i + \tilde{\lambda}N_{fl})\delta v(t) - \{\tilde{v}N_{\text{pch}} f(\tilde{\lambda}) + \tilde{v}^2(N_{f2} - N_{f1})\}\delta\lambda(t) + k_e\tilde{j}(z=1)\{2\tilde{\rho}_m(z=1)\delta j(t)$$
$$+ \tilde{j}(z=1)\delta\rho_m(z=1,t)\} + \int_{\tilde{\lambda}}^{1} \tilde{\rho}_m(z) L^m(\delta j(z,t))\, dz + \int_{\tilde{\lambda}}^{1} \tilde{S}_l(z)\delta\rho_m(z,t)\, dz \equiv L^f(\delta v(t)) = 0 \qquad [49]$$

where $\delta\lambda(t)$, $\delta j(z,t)$, $\delta\rho_m(z,t)$, $\tilde{S}_l(z)$, and L^m are given by [43], [44], [46], [40] and [39], respectively. For given heat flux shape $f(z)$, [49], which is a linear equation in $\delta v(t)$, can be used to study the stability of the fixed points. The solution of [49] using the Laplace transform, can be written in the form

$$\overline{\delta v}(s) = \frac{F^f(s)}{Q^f(s)} \qquad [50]$$

where the superscript f signifies the axial heat flux shape. The stability of fixed points (or steady-state solutions) is determined by the zeros of $Q^f(s)$. The function $Q^f(s)$ also can be obtained simply by assuming an explicit solution for $\delta v(t)$ of the form

$$\delta v(t) = e^{st}.$$

First, expressions for $\delta\lambda(t)$, $\delta j(t)$, and $\delta\rho_m(z, t)$ are simplified using the explicit expression for $\delta v(t)$. These simplified expressions are then substituted into [49], which yields the characteristic equation in the form

$$Q^f(s) = 0.$$

Roots of the characteristic equation for given set of parameter values, determine the stability of fixed points.

RESULTS AND DISCUSSION

The analysis so far has been carried out for a general, smooth axial heat flux shape $f(z)$. Now, to study the effects of two humps in the axial heat flux on the stability characteristics of the two-phase flow heated channel, a heat flux shape $f(z)$ of the form

$$f(z) = \sin(a + bz) + \alpha \sin(a + 3bz) \qquad [51]$$

is used, where a, b and α are constants. These constants allow very wide range of axial heat flux shapes—including those double-humped heat flux shapes that occur in operating BWRs—to be simulated and studied. [To compare the results with uniformly heated channels, we take $b = \alpha = 0$ and $a = \pi/2$.] Though for certain $\alpha \neq 0$, this choice of $f(z)$ yields, as desired, a double-humped heat flux profile, it also makes it necessary that few integrals in the characteristic equation be evaluated numerically. In fact, even the position of the boiling boundary at steady-state $\bar{\lambda}$, must be determined numerically by solving a transcendental equation, [24].

Results of the stability analysis are presented as stability boundaries in parameter space and in the form of a bifurcation diagram. Regions of parameter space where at least one root of the characteristic equation has positive real part are 'unstable', and regions where all roots of the characteristic equation are strictly negative are 'stable'. The three operating parameters in this problem are subcooling number N_{sub}, total phase change number $N_{pch,tot}$ and externally imposed pressure drop ΔP_{ex}. Setting values for the three operating parameters in the steady-state problem results in one or more possible solutions for inlet velocity and other dependent variables, called fixed point, which may or may not be stable. Hence, stability boundaries can be drawn in the three-dimensional parameter space $N_{sub} - N_{pch,tot} - \Delta P_{ex}$, (or any one of its two-dimensional projections) that separate stable regions in operating parameter space from unstable regions, i.e. regions in parameters space where the corresponding fixed points are stable from regions where the corresponding fixed points are unstable. Therefore, the projection of this stability boundary, for example on the $N_{sub} - N_{pch,tot}$ parameter space, should be for a constant externally imposed pressure drop ΔP_{ex} and hence, each point on the projected boundary should correspond to a different fixed point (different steady-state inlet velocity). Practical considerations, on the other hand, require stability boundaries to be presented for constant flow rate. An early experimental study of two-phase instabilities (Saha *et al.* 1976) was carried out for constant inlet flow rate, and data was presented in $N_{sub} - N_{pch}$ space for constant inlet velocity rather than for constant external pressure drop. Hence, the results of stability analyses, to be able to compare with the experimental data, also have been traditionally evaluated and presented for constant inlet velocity case. This is achieved by allowing different values of ΔP_{ex} along the stability boundary such that the combination of N_{sub}, $N_{pch,tot}$ and ΔP_{ex} always results in the same fixed inlet velocity for the entire stability boundary (Saha *et al.* 1976). Hence, the total pressure drop in the channel at each point on the stability boundaries, later presented in $N_{pch,tot} - N_{sub}$ space, is such that the combination of the three parameters results in a constant inlet velocity ($\tilde{v}_i = 1.0$). In this paper the results of the stability analysis in $\tilde{v} - N_{sub}$ space for fixed $N_{pch,tot}$, obtained by allowing different values of ΔP_{ex} along the stability boundary, also are presented.

Figure 2 shows five different heat flux shapes. For heat flux shapes A, B, C and D, $a = 0, b = \pi$, and $\alpha = 0.0$, 0.1, 0.2, 0.3, respectively. Figure 3 shows five stability boundaries in $N_{pch,tot} - N_{sub}$ space corresponding to the symmetric heat flux profiles shown in figure 2. A comparison of stability boundaries for the single-humped profile (case A) with flat heat flux profile (case E) shows that

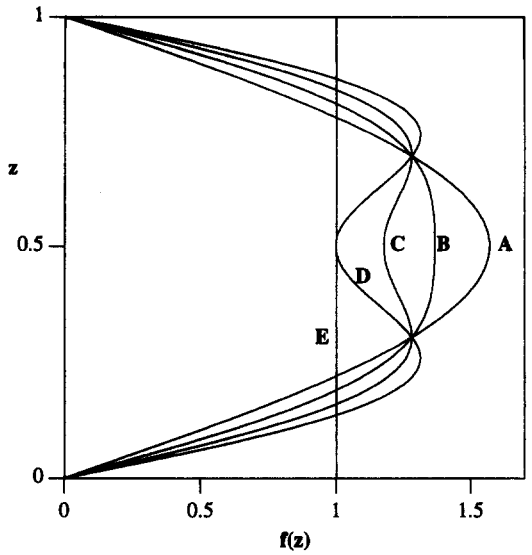

Figure 2. Five symmetric heat flux profiles. For cases A, B, C and D, $a = 0$, $b = \pi$ and $\alpha = 0.0, 0.1, 0.2, 0.3$ [51]. For case E, $f(z) = 1$.

channel A is more stable than channel E for low values of N_{sub} and less stable for high values of N_{sub}. For $\alpha = 0.1$ (case B) the heat flux flattens near the channel center, and compared to case A ($\alpha = 0.0$), the channel becomes less stable for low N_{sub} and more stable for large N_{sub} values. The trend continues as a "dip" develops in the heat flux profile near the center and the two peaks become distinct (cases C and D).

Comparing cases A, D, and E, it is clear that the stability characteristics of a channel with a symmetric double-humped heat flux profile are more similar to the channel with uniform heat flux

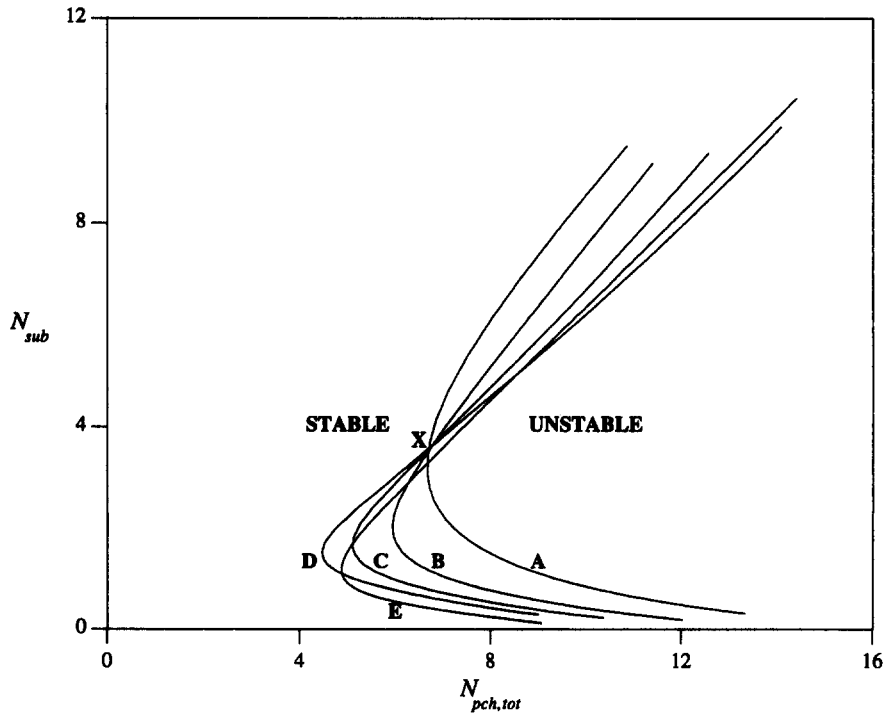

Figure 3. Stability boundaries that divide the parameter space into stable and unstable regions in $N_{pch,tot} - N_{sub}$ space for symmetric heat flux profiles shown in figure 2.

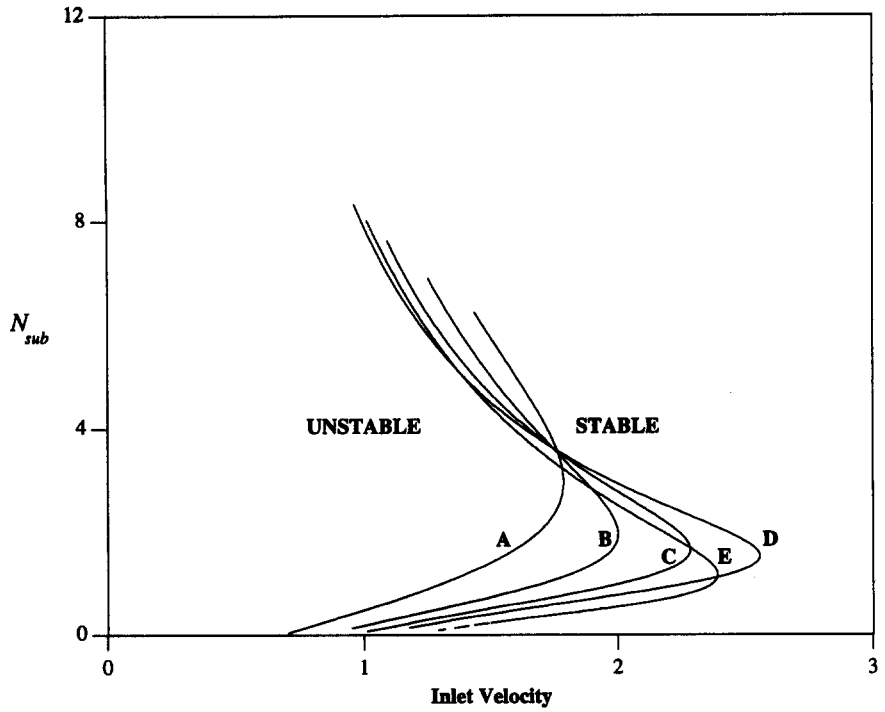

Figure 4. Stability boundaries in $\tilde{v} - N_{sub}$ space for symmetric heat flux profiles shown in figure 2.

than to a channel with a single hump. This effect is easily explained by the fact that for same total heat flux, double-humped heat flux profile is relatively "flatter" near the center and hence closer to the flat heat flux profile than the single-humped profile. An interesting feature to be noticed is that stability boundaries for cases A, B, C and D all pass through a common point, X. The point corresponds to values of N_{sub} and $N_{pch,tot}$ that result in a boiling boundary at the center of the heated channel. Boiling boundary is in the lower (upper) half of the channel for all points in $N_{pch,tot}$–N_{sub} parameter space below (above) the straight line that passes through the origin and the point X. It is clear that whether the channel is more or less stable due to a second hump depends upon the location of the boiling boundary. The second hump, which makes the flux profile relatively flatter,

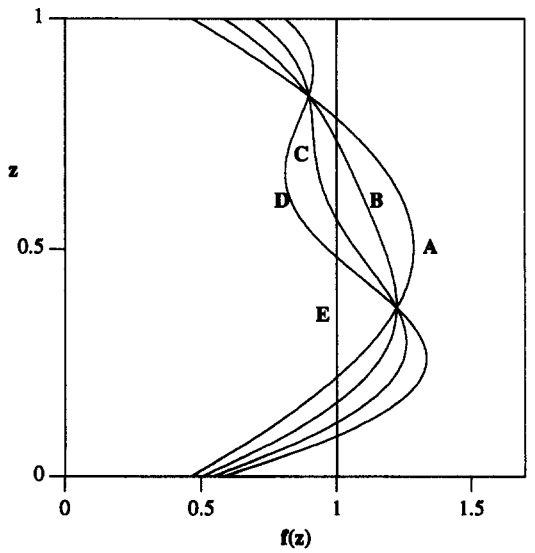

Figure 5. Asymmetric heat flux profiles. For cases A, B, C and D, $a = 0.37$, $b = 2.4$ and $\alpha = 0.0, 0.1, 0.2, 0.3$ [51]. For case E, $f(z) = 1$.

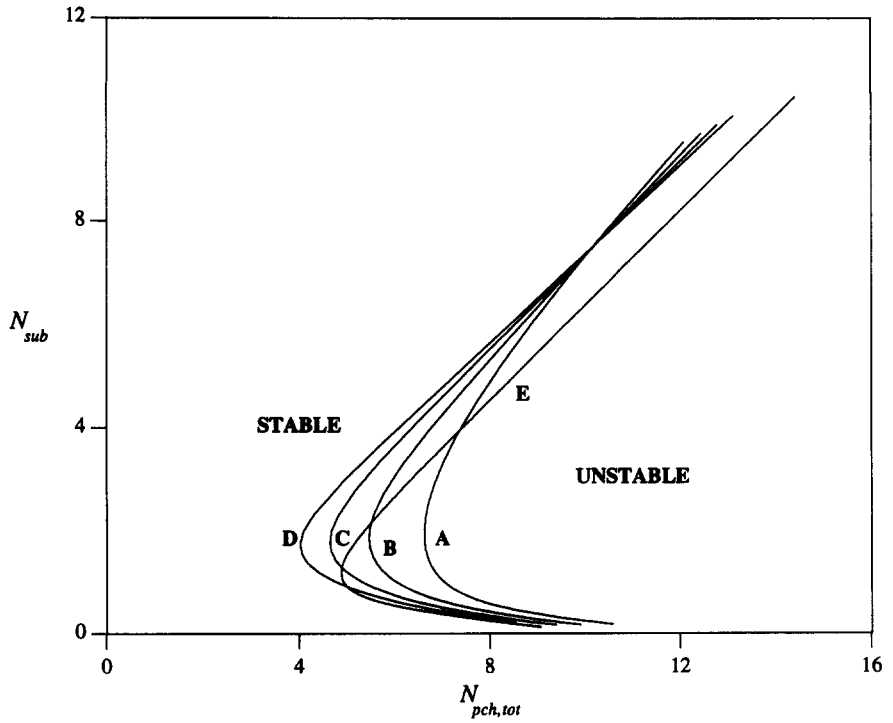

Figure 6. Stability boundaries that divide the parameter space into stable and unstable regions in $N_{pch,tot} - N_{sub}$ space for asymmetric heat flux profiles shown in figure 5.

makes a channel less stable (compared to a single-humped channel) if the boiling boundary is in the lower half of the channel, and more stable if the boiling boundary is in the upper half of the channel. This is physically understandable since the effect of the second hump on the boiling-boundary is opposite for the two cases. The boiling boundary moves down, hence increasing the

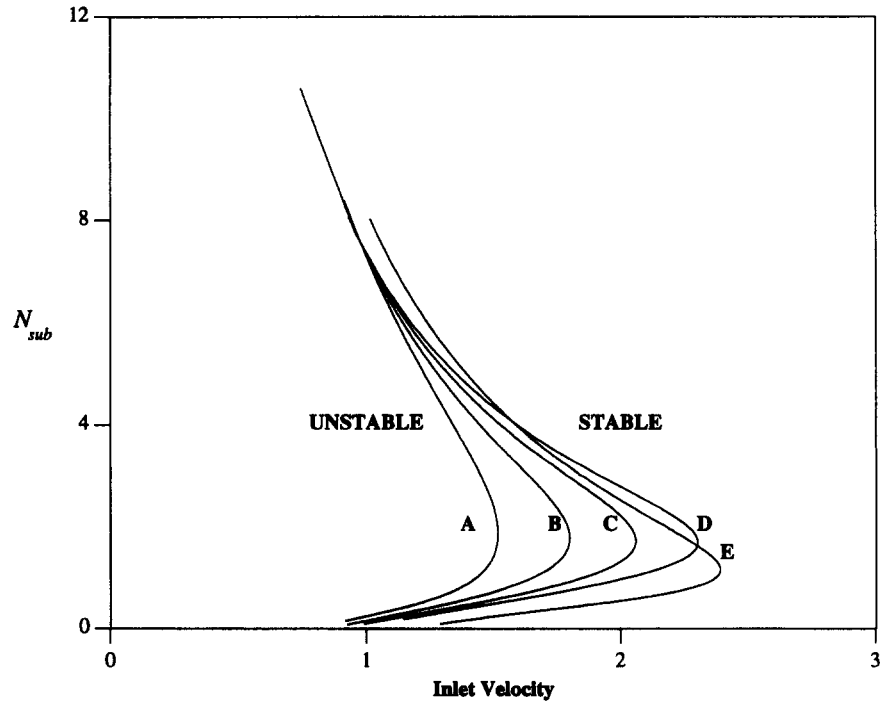

Figure 7. Stability boundaries in $\tilde{v} - N_{sub}$ space for asymmetric heat flux profiles shown in figure 5.

length of the two-phase region, due to the second hump if it (the boiling boundary) is in the lower half of the channel. Whereas, it moves up (decreasing the length of the two-phase region) if the boiling boundary for the single-humped case is in the upper half of the heated channel. Results of the stability analysis are presented in $\tilde{v}$–N_{sub} plane in figure 4. Here again, as expected, the stable region for low N_{sub} increases as the second hump appears in the axial heat flux distribution.

To analyze more realistic axial heat flux profiles that are found in practical engineering equipment like BWRs, the stability of two-phase flow heated channels with two *asymmetric* peaks in axial heat flux has also been studied. Figure 5 shows the heat flux shapes for $a = 0.37$, $b = 2.4$, and $\alpha = 0.0$, 0.1, 0.2 and 0.3. The general trends for the stability characteristics of the asymmetric axial heat flux profile, as shown in figures 6 and 7, are the same as found in the symmetric heat flux variation case. Compared with the symmetric heat flux profile, in this asymmetric case, the region of parameter space where the channel becomes *less* stable due to the appearance of a second hump is significantly larger than the region where the second hump makes the channel *more* stable.

Results, both for the symmetric and asymmetric, double-humped axial heat flux variation cases presented above, clearly show that a channel with double-humped heat flux variation can be significantly more unstable when compared with another channel with same total heat supplied (same $N_{pch,tot}$) but uniform heat flux or one with single-humped heat flux variation. For example, comparison of stability characteristics of channels D (a very realistic bottom-peaked, double-humped axial heat flux), A (single-humped symmetric axial heat flux) and E (uniform heat flux) shown in figure 5 shows that channel D is less stable than channel A for almost the entire practically relevant region of the parameter space ($N_{sub} \lesssim 8$), whereas channel D is less stable than channel E for $0.5 \lesssim N_{sub} \lesssim 8$ (see figure 6). Obviously any application of stability analyses developed for

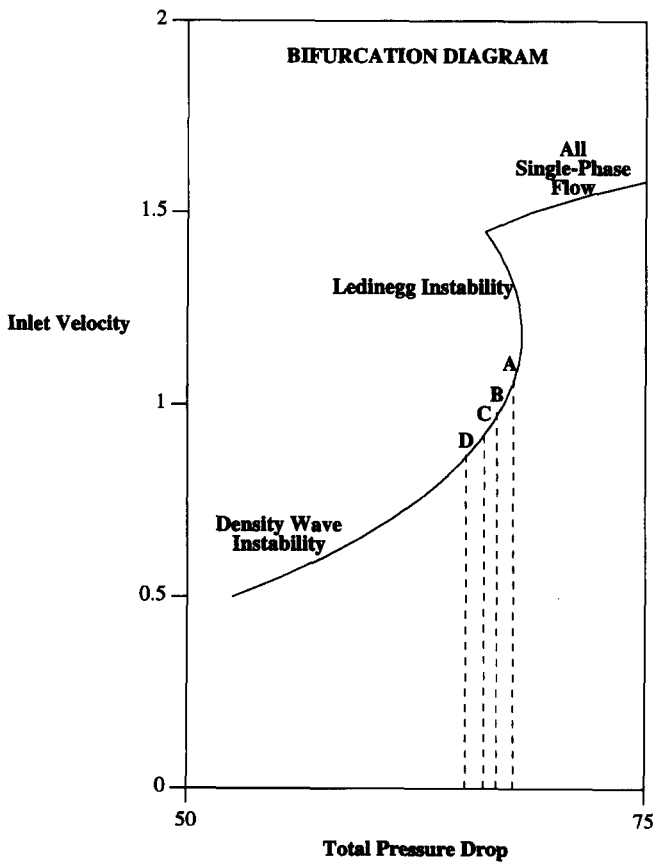

Figure 8. Bifurcation diagram for the axially symmetric heat flux profiles shown in figure 2. Channels A, B, C and D become unstable as the total pressure drop—while keeping N_{sub} and $N_{pch,tot}$ fixed at 4.76 and 7.0, respectively—is decreased below the corresponding critical value $\Delta P_{ex,crit}$, indicated by the dashed vertical lines for these cases. (Since the difference between the steady-state characteristic curves for different cases is extremely small, to keep the figure uncluttered only a single curve is drawn.)

uniformly heated channels or those developed for channels with single-humped axial flux variation, to channels with realistic double-humped axial heat flux shapes can lead to very non-conservative results.

Results in the form of a bifurcation diagram are presented in ΔP_{ex}–$\tilde{v}$ plane, which, for all other parameters fixed, shows the characteristic inlet velocity dependence and its stability on externally imposed pressure drop. Figures 8 and 9 show the characteristic curves for the heat flux shapes shown in figures 2 and 5, respectively. [Although there is a unique characteristic curve for each of the flux shapes in figures 2 and 5, the difference between these curves is relatively small and when drawn on the same scale they form a single 'thick' curve. Hence, to keep the figures uncluttered we only have drawn one characteristic curve in figures 8 and 9.] As is well known, the middle branch of the characteristic curve is unstable due to Ledinegg instability. The lower branch of the S-shaped curve is unstable due to oscillatory instabilities for values of the bifurcation parameter, external pressure drop, less than a critical value $\Delta P_{ex,crit}$. It has been shown for uniformly heated channels that this instability is a result of supercritical Hopf bifurcation (Achard *et al.* 1985; Rizwan-uddin & Dorning 1986) and hence, stable limit cycle solutions exist in a finite range of external (or total) pressure drop values less than $\Delta P_{ex,crit}$ (Rizwan-uddin 1987).

The effect of the second hump on the bifurcation diagram for the same parameter values can be different for the symmetric and asymmetric axial heat flux cases. Shown in figures 8 and 9 are the values of the bifurcation parameter $\Delta P_{ex,crit}$ for different heat flux shapes for inlet subcooling $N_{sub} = 4.76$ and $N_{pch,tot} = 7$. The channel becomes unstable for external pressure drop less than $\Delta P_{ex,crit}$. For parameter values used here, bifurcation occurs at lower values of the bifurcation parameter ΔP_{ex}, i.e. $\Delta P_{ex,crit}$ decreases as the single-humped heat flux profile (case A) is replaced by a *symmetric* double-humped heat flux profile (case D). See figure 8. For the same parameter

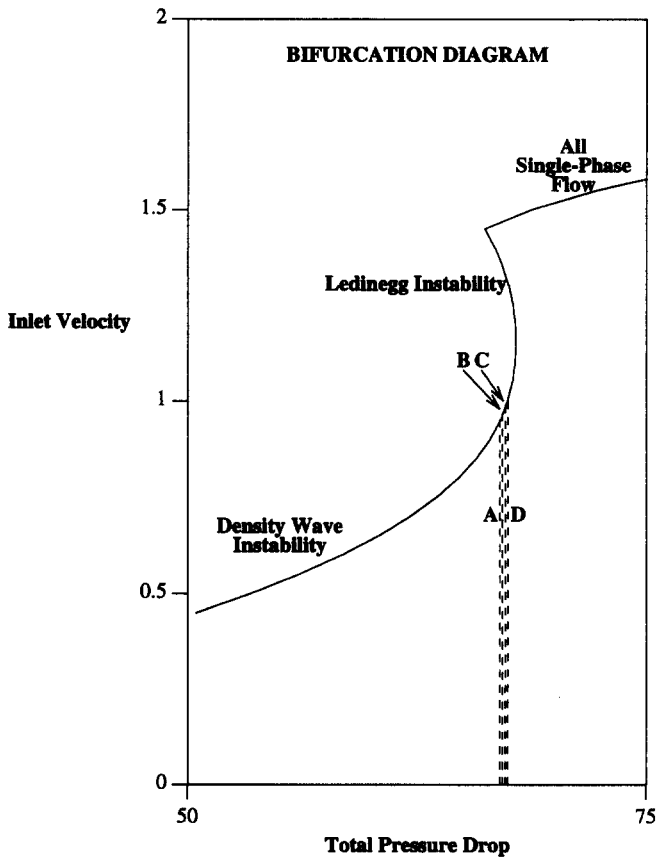

Figure 9. Bifurcation diagram for the axially asymmetric heat flux profiles shown in figure 5. Channels A, B, C and D become unstable as the total pressure drop—while keeping N_{sub} and $N_{pch,tot}$ fixed at 4.76 and 7.0, respectively—is decreased below the corresponding critical value $\Delta P_{ex,crit}$, indicated by the dashed vertical lines for these cases.

values, the trend is opposite for the *asymmetric* double-humped axial heat flux profile. In this case, bifurcation occurs at higher values of the bifurcation parameter for double-humped heat flux shapes (case D) than for the single-humped case (case A). Although the parameter values for figures 3 and 6 are different from those used in figure 8 (and 9), the same trend can actually be seen also in figures 3 and 6. For $N_{sub} = 5$ and $N_{pch,tot} = 9$, figure 3 shows that the channel with symmetric double-humped heat flux profile (case D) is more stable than the single-humped profile case (case A). For the same parameter values, figure 6 shows that the channel with asymmetric double-humped axial flux distribution is less stable (case D) than the channel with single-humped heat flux profile (case A).

Also to be remembered is the fact that the stability characteristics of heated channels with two-phase flow described above are actually a function both of the heat flux shape and the parameter values. For example, for $N_{sub} = 1.0$ (and $N_{pch,tot} = 8$), even the channel with symmetric double-humped heat flux shape, similar to the asymmetric case, is less stable (case D) than the channel with a single-humped heat flux profile (case A). See figure 3. In other words, bifurcation even for the symmetric double-humped heat flux shape, occurs at higher total pressure drop than the critical value for the single-humped case, if the subcooling number N_{sub} is small.

CONCLUSIONS

Stability analysis of two-phase flow heated channels with double-humped axially varying heat flux has been carried out. The effect of different axial heat flux shapes on channel stability is found to be different for channels operating in different regions of the parameter space. For example, as the heat flux shape is changed from a single-humped profile to a symmetric double-humped profile, a channel with low inlet subcooling becomes less stable, while a channel with high inlet subcooling becomes more stable.

Importance of the boiling boundary dynamics in the stability analysis of two-phase flow has once again been established. The channel becomes less stable by the introduction of a different axial heat flux profile if it results in increasing the two-phase region length, i.e. if the steady-state boiling boundary location moves down. The results presented here are useful in the analysis of realistic two-phase flow heated systems, such as the boiling water nuclear reactors, which have been found to have double-humped variations in their axial heat flux profile under certain operating conditions.

Acknowledgement—This paper was prepared with the support of the U.S. Nuclear Regulatory Commission (NRC) under grant No. NRC-04-90-113. The opinions, findings, conclusions and recommendations expressed herein are those of the author and do not necessarily reflect the views of the NRC.

REFERENCES

ACHARD, J.-L., DREW, D. A. & LAHEY, R. T., JR. 1985 The analysis of nonlinear density-wave oscillations in boiling channels. *J. Fluid Mech.* **155,** 213–232.

ARAYA, F., YOSHIDA, K., HIRANO, M. & YABUSHITA, Y. 1991 Analysis of a neutron flux oscillation event at LaSalle-2. *Nucl. Tech.* **93,** 82–91.

BERGDAHL, B. G., REISCH, F., OGUMA, R., LORENZEN, J. & ÅKERHIELM, F. 1989 BWR stability investigation at Forsmark I. *Ann. Nucl. Energy* **16,** 509–520.

BOURÉ, J. A., BERGLES, A. E. & TONG, L. S. 1973 Review of two-phase flow instability. *Nucl. Eng. Des.* **25,** 165–192.

BOURÉ, J. A. 1978 Oscillatory Two-Phase Flows. In *Two-Phase Flows and Heat Transfer with Application to Nuclear Reactor Design Problems.* (Edited by Ginoux, J. J.). Hemisphere, New York.

CLAUSE, A., LAHEY, R. T., JR & PODOWSKI, M. 1989 An analysis of stability and oscillation modes in boiling multichannel loops using parameter perturbation methods. *Int. J. Heat Mass Transfer* **32,** 2055–2064.

DIEDERICH, G. J. 1988 Potentially significant event: Unit 2 scram initiated by valving error. LaSalle County Station, Commonwealth Edison Company, letter to N. Kalivianakis.

FRUTERA, M. 1986 Validity of homogeneous flow model for instability analysis. *Nucl. Engng Des.* **95,** 65–77.

LORENZINI, E. 1981 A simplified method proposal for practical determination of aperiodic two-phase flow instability. *Int. J. Multiphase Flow* **7,** No. 6, 635–645.

RIZWAN-UDDIN 1987 Two-phase flow instability. In *Third Proc. of Nuclear Thermal Hydraulics*, pp. 123–130. American Nuclear Society, La Grange Park, Illinois.

RIZWAN-UDDIN & DORNING, J. J. 1986 Some nonlinear dynamics of a heated channel. *Nucl. Engng Des.* **93,** 1–14.

RIZWAN-UDDIN & DORNING, J. J. 1987 Nonlinear stability analysis of density-wave oscillations in nonuniformly heated channels. *Trans. Am. Nucl. Soc.* **54,** 172.

RIZWAN-UDDIN & DORNING, J. J. 1988 A chaotic attractor in a periodically forced two-phase flow system. *Nucl. Sci. Engng* **100,** 393–404.

SAHA, P., ISHII, M. & ZUBER, N. 1976 An experimental investigation of thermally induced flow oscillations in two-phase systems. *J. Heat Transfer* **98,** 616–622.

SANDOZ, S. A. & CHEN, S. F. 1983 Vermont yankee stability tests during cycle 8. *Trans. Am. Nucl. Soc.* **45.**

STENNING, A. H. & VEZIROĞLU, T. N. 1965 Flow oscillation modes in forced convection boiling. *Proc. 1965 Heat Transfer and Fluid Mechanics Inst.*, pp. 301–316. Stanford Univ. Press, Calif.

ÜNAL, H. C. 1981 Density-wave oscillations in sodium heated once-through steam generator tubes. *J. Heat Transfer* **103,** 485–491.

VALTONEN, K. 1989 BWR stability analysis. Technical Report 1022, Finnish Centre for Radiation and Nuclear Safety, Helsinki.

WULFF, W., CHENG, H. S., MALLEN, A. N. & ROHATGI, U. S. 1991 BWR stability analysis with the BNL engineering plant analyzer. NUREG/CR-5816 Brookhaven National Laboratory.

XIAO, M., CHEN, X. J., ZHANG, M. Y., VEZIROĞLU, T. N. & KAKAÇ, S. 1993 A multivariable linear investigation of two-phase flow instabilities in parallel boiling channels under high pressure. *Int. J. Multiphase Flow* **19,** 65–77.

ZUBER, N. & FINDLEY, J. A. 1965 Average volumetric concentration in two-phase flow systems. *J. Heat Transfer* **87,** 443–468.

ZUBER, N. & STAUB, F. W. 1967 An analytical investigation of the transient response of the volumetric concentration in a boiling forced flow system. *Nucl. Sci. Engng* **30,** 268–278.

APPENDIX A

The Dimensionless Variables and Parameters

The single- and two-phase region equations are made dimensionless using the dimensional channel length L^*, liquid density ρ_L^*, latent heat Δh_{LG}^*, and an arbitrary characteristic velocity v_0^*. The dimensionless variables and parameters that appear in these equations are defined as follows:

$$j = \frac{j^*}{v_0^*}, \quad v_i = \frac{v_i^*}{v_0^*}, \quad z = \frac{z^*}{L^*},$$

$$\lambda = \frac{\lambda^*}{L^*} \quad t = \frac{t^*}{L^*/v_0^*}, \quad \rho_m = \frac{\rho_m^*}{\rho_L^*},$$

$$h_m = \frac{h_m^*}{\Delta h_{LG}^*}, \quad P = \frac{P^*}{\rho_L^* v_0^{*2}}, \quad Fr = \frac{v_0^{*2}}{g^* L^*},$$

$$N_\rho = \frac{\rho_G^*}{\rho_L^*}, \quad N_r = \frac{\rho_L^*}{\Delta\rho^*}, \quad N_p = 1 - \frac{1}{N_r},$$

$$N_{f1} = \frac{f_s^* L^*}{2D^*}, \quad N_{f2} = \frac{f_m^* L^*}{2D^*}, \quad N_{sub} = \frac{\Delta h_i^* \Delta\rho^*}{\Delta h_{LG}^* \rho_G^*},$$

$$N_{pch} = \frac{q''^* \xi^* L^* \Delta\rho^*}{A^* \Delta h_{LG}^* \rho_G^* \rho_L^* v_0^*}$$